

Microstructural Study of a Mechanically Alloyed ODS Superalloy

M. Mujahid, C.A. Gater, and J.W. Martin

(Submitted 2 December, 1997; in revised form 4 March 1998)

Extruded bars of oxide-dispersion-strengthened (ODS) alloy MA-6000 have been annealed isothermally as well as in temperature gradients. The temperatures used for annealing produced secondary recrystallization in all the samples, although the final grain aspect ratio was different for each annealing process. Interrupted gradient anneal experiments showed a curved secondary recrystallization front, with the surface recrystallizing at a lower temperature than the interior. It is believed this is caused indirectly by the strain gradients arising during extrusion. Grain-orientation analysis of recrystallized material revealed that a $\langle 110 \rangle$ fiber texture is present. A progressive grain reorientation toward $\langle 110 \rangle$ has been measured behind the recrystallization front using microbeam electron diffraction. In addition, changes in the distribution, size, and morphology of different types of precipitates and particles occurring during various stages of annealing have also been studied. Grain-boundary pinning by the stable oxide particles plays an important role in determining the grain growth behavior at high temperatures.

Keywords annealing, grain growth, mechanical alloying, texture

1. Introduction

Since the initial introduction of superalloys to jet engines, much research has been directed toward improving the materials in order to meet the continual demand for increased power and longer engine lives with corresponding decreased maintenance. The majority of superalloys in use for jet engines are nickel-base and conventionally consist of a polycrystalline fcc γ matrix strengthened by the precipitation of $\gamma' \text{Ni}_3(\text{Al}, \text{Ti})$.

M. Mujahid, Faculty of Metallurgy and Materials Engineering, GIK Institute of Engineering Science and Technology, Topi, NWFP—23460, Pakistan; and C.A. Gater and J.W. Martin, Department of Materials, University of Oxford, Parks Road, Oxford OX1 3PH, UK. Contact e-mail: mujahid@giki.sdnpc.undp.org.

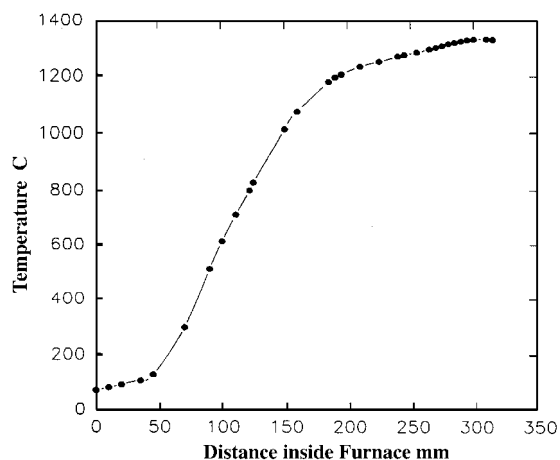


Fig. 1 Temperature profile within the body of zone-annealing furnace

Mechanical alloying is an effective way of producing oxide-dispersion-strengthened (ODS) alloys, and the technique has been employed to produce nickel-base superalloys that are strengthened by both the γ' phase and also dispersions of yttria (Ref 1). Enhancement of creep ductility of these materials is achieved if the matrix grain structure is of high aspect ratio (Ref 2), and this is usually brought about by a process of zone-annealing, which also produces a strong texture by secondary recrystallization (Ref 3).

The mechanisms by which the columnar grain structure and texture develop in zone-annealed ODS alloys are not fully understood. The object of the present work is to follow the development of microstructure and texture during the annealing of extruded MA-6000 bars using optical and electron microscopy techniques.

2. Experimental Materials and Methods

2.1 As-Received Material

The nominal composition of the alloy MA-6000 in weight percent is as follows:

- Nickel, 69%
- Chromium, 15%
- Molybdenum, 2%
- Tungsten, 4%
- Tantalum, 2%
- Aluminum, 4.5%
- Titanium, 2.5%
- Zirconium, 0.15%
- Boron, 0.01%
- Carbon, 0.05%
- Y_2O_3 , 1.1%

The specimens were in the form of hot-extruded bars with cylindrical (12 mm diameter) as well as rectangular (10 by 15 mm) cross sections.

2.2 Annealing Heat Treatments

Isothermal Annealing. The specimens (30 mm in length) for isothermal annealing, taken from round bars, were placed in a Carbolite furnace (Carbolite Inc., Watertown, WI) equipped with a programmable temperature controller. The controller was programmed to raise the furnace temperature to 1235 °C in 1 h. This temperature was maintained for 25 min after which the sample was air cooled to room temperature.

Static Gradient Annealing. This treatment was carried out, on round bar specimens, in a platinum resistance furnace with a built-in vertical temperature gradient, the details of which are described in Ref 4. Figure 1 shows the temperature profile obtained within the furnace tube when the controller is set at 1300 °C. The sample was placed in the furnace in such a way that the top surface was 280 mm inside the furnace. After holding at that point for 85 min the specimen was air cooled to room temperature.

Zone Annealing was carried out (on samples both round and rectangular extrusions) in the same platinum resistance furnace. Specimens were partially zone annealed at a traverse rate of 38 mm/h through the furnace (set at 1300 °C) to produce an interface in the sample. Three measuring thermocouples were used, located at the bottom, halfway along the length and at the top of the specimen. Each run was stopped when the middle thermocouple achieved the appropriate temperature; the furnace was then automatically reversed and the specimen allowed to air cool.

2.3 Electron Channelling Patterns

Selected-area channelling patterns (SACPs) were obtained on a JEOL 100C scanning transmission electron microscope (STEM; JEOL Ltd., Tokyo, Japan) at a rocking angle of $\pm 15^\circ$ from grains within recrystallized samples. This technique is particularly useful for scanning large areas of the specimens when the grains are larger than 10 μm in diameter. Specimens were prepared in transverse section, such that the electron beam was parallel to the extrusion axis in each specimen. By moving the electron beam across a specimen in a direction perpendicular to the direction of growth of the grains, it was possible to obtain a series of SACPs from a number of neighboring grains. Poles were then readily identified with the aid of a channelling map (Ref 5).

2.4 Grain Orientation Determination by TEM

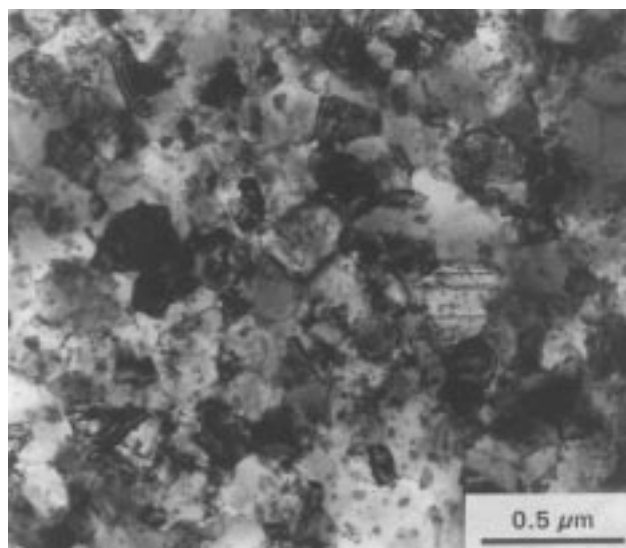
The grains in the as-received material and in the untransformed material behind the zoning interface were too small to be analyzed using the SACP technique. An electron diffraction technique was, therefore, employed on thin foil specimens (having foil plane normal to the extrusion axis) in the Philips CM20 transmission electron microscope (TEM; Philips Electron Optics, Eindhoven, Holland). Using the instrument in the diffraction mode, a spot size of 100 nm, and a camera length of 330 mm, a pattern could be produced from individual submicrometer-sized grains in the unrecrystallized material. The angular distance represented by the viewing screen was found to be approximately 10° . The poles in these patterns were again identified with the help of a Kikuchi map. Several hundred grains in each specimen were analyzed using this method. The

population of $\langle 110 \rangle$ grains was determined by positioning the foils, with respect to the beam, at 0° (i.e., no tilt) and 10° tilt. Tilting the foils by 10° was intended to bring a further cone of observation into view, providing an opportunity to determine the population of grains lying up to 20° away from the extrusion axis.

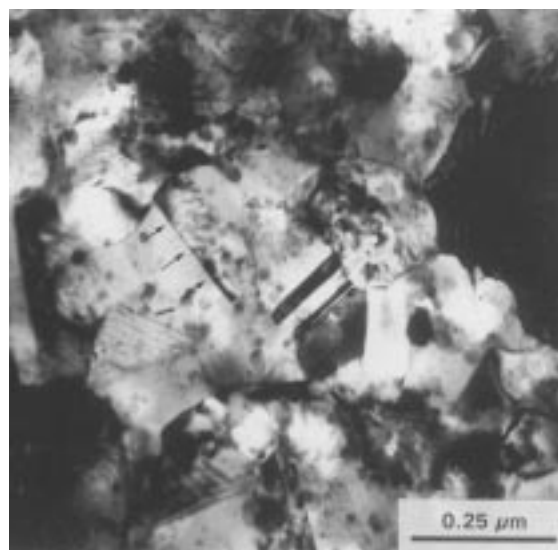
3. Experimental Results

3.1 As-Extruded Material

Transmission electron microscopy revealed an equiaxed grain structure with an average grain diameter of 0.2 μm (Fig. 2). A very low dislocation density within the grains suggests that primary recrystallization has occurred during



(a)



(b)

Fig. 2 TEM micrographs showing microstructure in the as-extruded material. (a) Grain size of 0.2 μm . (b) Twins in the grains pointed by arrows

hot extrusion. Twins were also observed to be present in a large number of grains. Microbeam electron diffraction in the TEM revealed that a majority of the grains analyzed had an orienta-

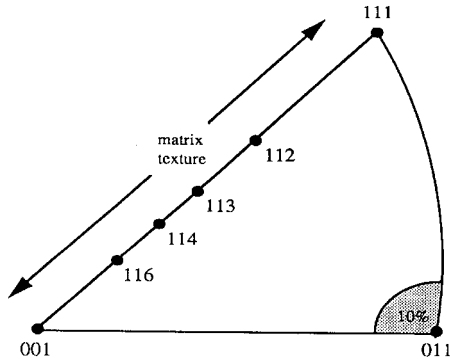


Fig. 3 Schematic of standard triangle showing the “matrix” texture of as-received material along the extrusion axis. Majority of the grains lie within $\langle 111 \rangle$ and $\langle 001 \rangle$.

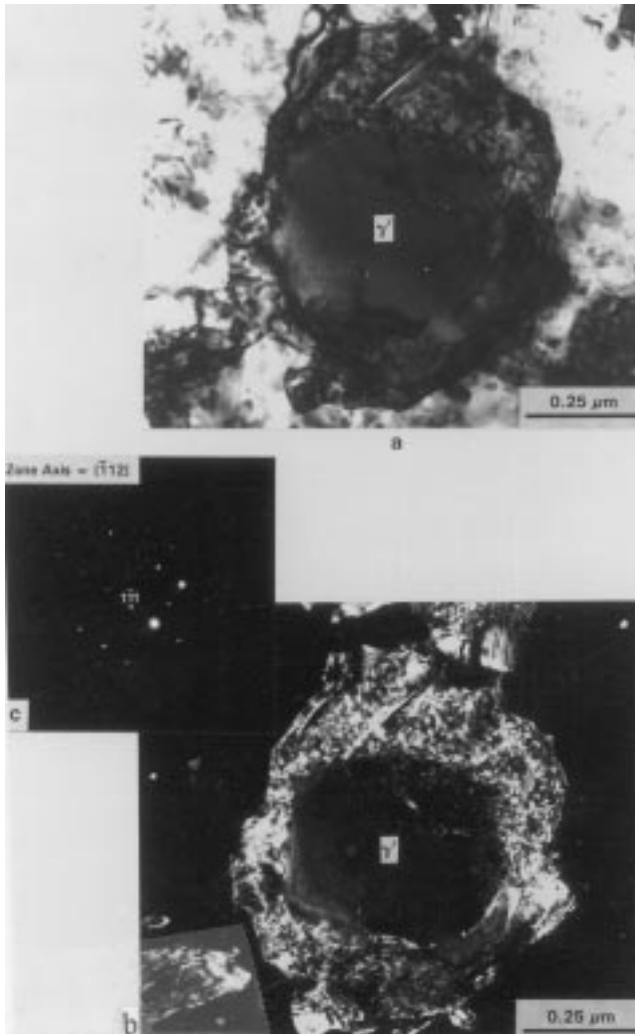


Fig. 4 TEM micrograph of a large γ -precipitate in the as-received material. (a) BF. (b) DF. (c) Diffraction pattern showing the spot used for DF

tion within the $\langle 001 \rangle$ to $\langle 111 \rangle$ band parallel to the extrusion axis (Fig. 3), and approximately 10 to 15% of the grains had the $\langle 110 \rangle$ direction parallel to the extrusion axis (within 10°). The results of some of these analyses are given in Table 1.

The size and distribution of γ particles vary considerably in the as-extruded material. Some particles are seen to be as large as the grain itself (Fig. 4), while certain grains had several γ particles in them. Scanning electron micrograph (SEM) in Fig. 5 shows a typical distribution of coarse irregular γ particles with a size range of 0.1 to 0.3 μm , although some particles as small as 50 nm and some rare ones as large as 0.5 μm are also observed.

The oxide dispersion was examined using TEM, which showed that they are distributed randomly with an average diameter of 5.5 nm.

3.2 Isothermally Annealed Material

Longitudinally sectioned specimens (Fig. 6) revealed that the initial fine grain structure was transformed to a large elongated grain structure. The grains were always seen to have grown more along the extrusion axis (~ 1 to 2 mm in length) than in the transverse direction (~ 0.5 mm in diameter). A SACP analysis showed a common $\langle 110 \rangle$ direction aligned parallel to

Table 1 Population of $\langle 110 \rangle$ grains in tilted and untilted TEM thin foils

0 tilt		10° tilt	
Fraction of $\langle 110 \rangle$ grains	Percentage of $\langle 110 \rangle$ grains	Fraction of $\langle 110 \rangle$ grains	Percentage of $\langle 110 \rangle$ grains
$\frac{3}{15}$	20	$\frac{1}{17}$	6
$\frac{4}{21}$	19	$\frac{1}{20}$	5
$\frac{1}{20}$	5	$\frac{1}{20}$	5
$\frac{3}{20}$	15	$\frac{2}{20}$	10
$\frac{3}{20}$	15	$\frac{1}{20}$	5
Total:			
$\frac{14}{96}$	15	$\frac{6}{97}$	7

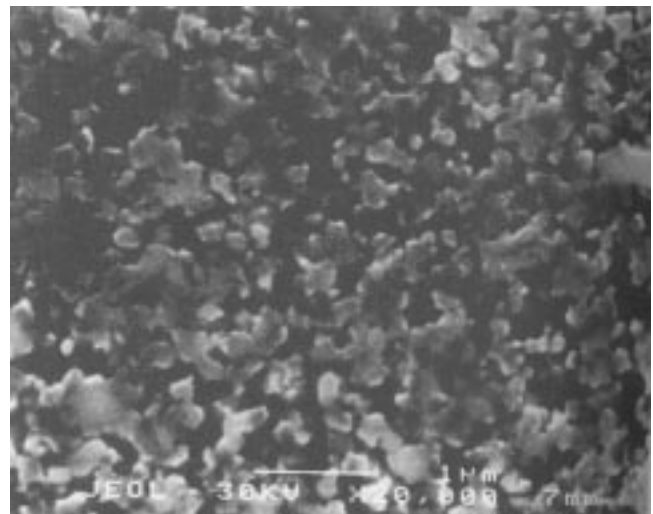


Fig. 5 SEM micrograph showing the size and morphology of γ -phase in the as-received material

the extrusion axis. It seems that the microstructure develops by secondary recrystallization because only a few grains having similar orientations grow in an abnormal fashion while consuming all the rest in the process.

3.3 Material Annealed in Static Temperature Gradient

The gradient observed in the 60 mm long specimen was approximately 3 °C/mm. A macrophotograph of a longitudinally sectioned specimen (Fig. 7) shows secondary recrystallized grains as well as untransformed regions with a diffuse and curved interface between them. The curved interface implies that the transformation temperature is higher in the center as compared to the surface of the bars. The minimum temperature at which the grains grow abnormally at the interface was found to be ~1160 °C.

The grains in the transformed region were observed to have elongated along the extrusion axis (i.e., parallel to the temperature gradient). The number of grains across the cross section is larger near the top surface as compared to near the interface. The aspect ratio of the topmost grains is low, but increases as the interface is approached. This behavior suggests that the grains, which can nucleate and grow at a lower temperature have higher mobility. The aspect ratio of these elongated grains

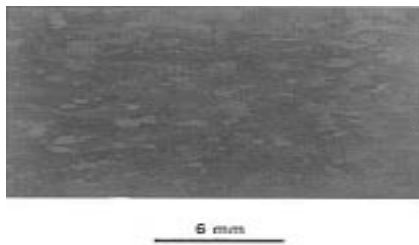


Fig. 6 Optical macrophotograph of isothermally annealed round cross-section specimen

was much higher compared with the aspect ratio of the grains found in isothermally annealed samples.

The SACP analysis in the SEM again revealed the presence of a strong <110> texture along the axis of the bars.

3.4 Zone-Annealed Material

Transformed Region. Macrophotographs of longitudinally sectioned specimens, which have been partially zone annealed, are shown in Fig. 8. The temperature gradient along the axis of the specimens was observed to be ~4 °C/mm. Grains of high aspect ratio are seen across the entire cross section in the transformed region, and a curved transformation (zoning)

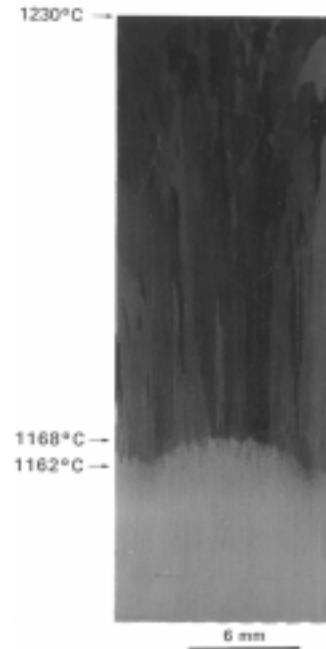


Fig. 7 Optical macrophotograph of round cross-section specimen, sectioned longitudinally after annealing in a stationary temperature gradient

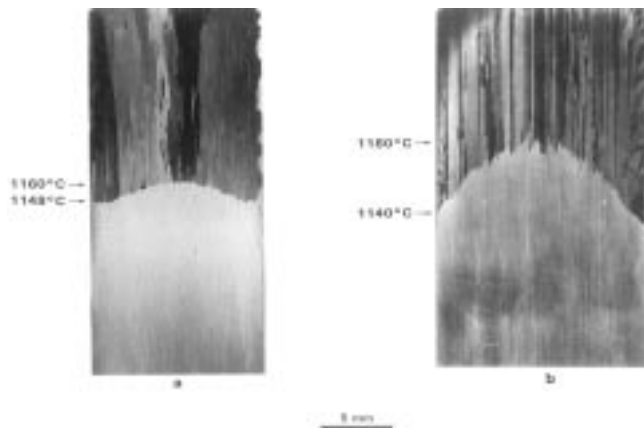


Fig. 8 Optical macrophotographs of longitudinal section of partially zone-annealed specimens. (a) Round cross section. (b) Rectangular cross section

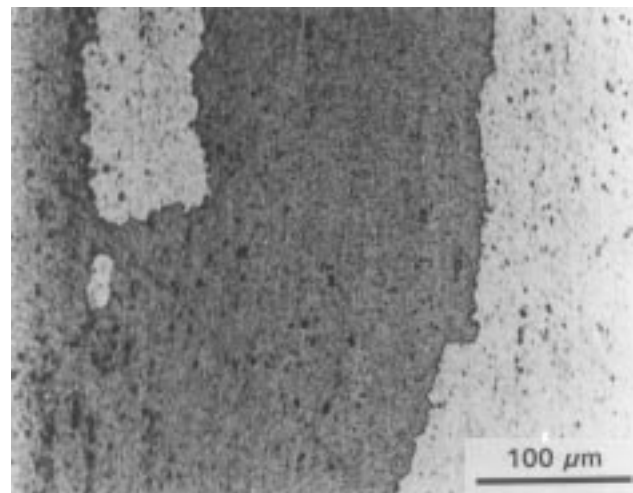


Fig. 9 Optical micrograph showing serrated grain-boundary structure in the recrystallized region of specimen shown in Fig. 8

interface is again observed. Closer examination of the transformed material revealed that the grain boundaries were not straight but highly serrated (Fig. 9) The zoning interface in round bars was observed to be growing at $\sim 1160^\circ\text{C}$. In the case of rectangular bars, the temperature of transformation was $\sim 1140^\circ\text{C}$ at the surface and $\sim 1180^\circ\text{C}$ in the interior. The SACP analysis of the transformed grains showed that their longitudinal axis was aligned close to $\langle 110 \rangle$, that is, within 5° .

Untransformed Region. The TEM studies on the material behind the zoning interface showed a consistent grain size of $0.4\mu\text{m}$. In addition, grains were counted as having a $\langle 110 \rangle$ orientation if their orientations were within 10° of $\{110\}$ pole. Figure 10 shows that the number of $\langle 110 \rangle$ grains progressively increases as one passes up the temperature gradient approaching the zoning interface. This indicates that a reorientation of the grains toward $\langle 110 \rangle$ may be taking place. In addition, $\langle 110 \rangle$ grains were usually observed to occur in groups of two or more, rather than in isolation (Fig. 11). The remaining “matrix” texture in this regime (close to the zoning interface), shown in Fig. 12, was still between $\langle 100 \rangle$ and $\langle 111 \rangle$ with more grains close to $\langle 112 \rangle$. The γ' size and morphology in the transformed as well as in the unrecrystallized material is shown in Fig. 13.

4. Discussion of Results

The results have shown that all three kinds of annealing heat treatments performed on alloy MA-6000 samples produced microstructures with very large grains and with a strong $\langle 110 \rangle$ texture, which is generated along the axis of the bars. The only difference was the aspect ratio of the grains, which was maximum in the case of zone annealing and minimum for isothermal annealing. Static gradient annealing also produced grains with higher aspect ratio compared with isothermally annealed samples. The exaggerated grain growth of selectively oriented grains is believed to occur by a process of secondary recrystallization. The mechanisms involved in the development of microstructure during zone annealing are discussed in the fol-

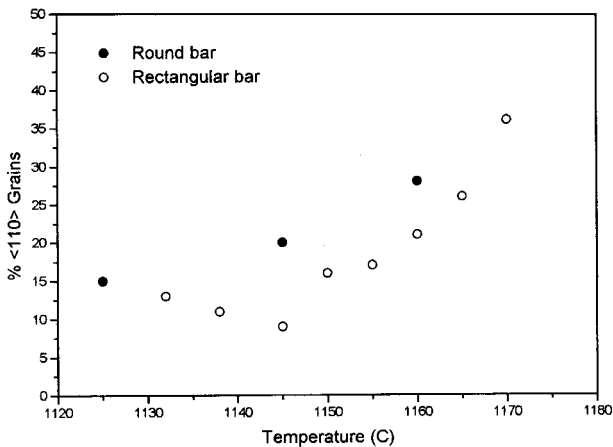


Fig. 10 Graph showing the population of $\langle 110 \rangle$ grains behind the zoning interface in partially zone-annealed specimens as a function of temperature

lowing subsections by looking at the material behind the interface more closely.

4.1 Effect of Particles on Normal Grain Growth

As the material passes up the temperature gradient, uniform (or normal) grain growth occurs from an average size of 0.2 to $0.4\mu\text{m}$. The grain size remains constant at $\sim 0.4\mu\text{m}$ up to the

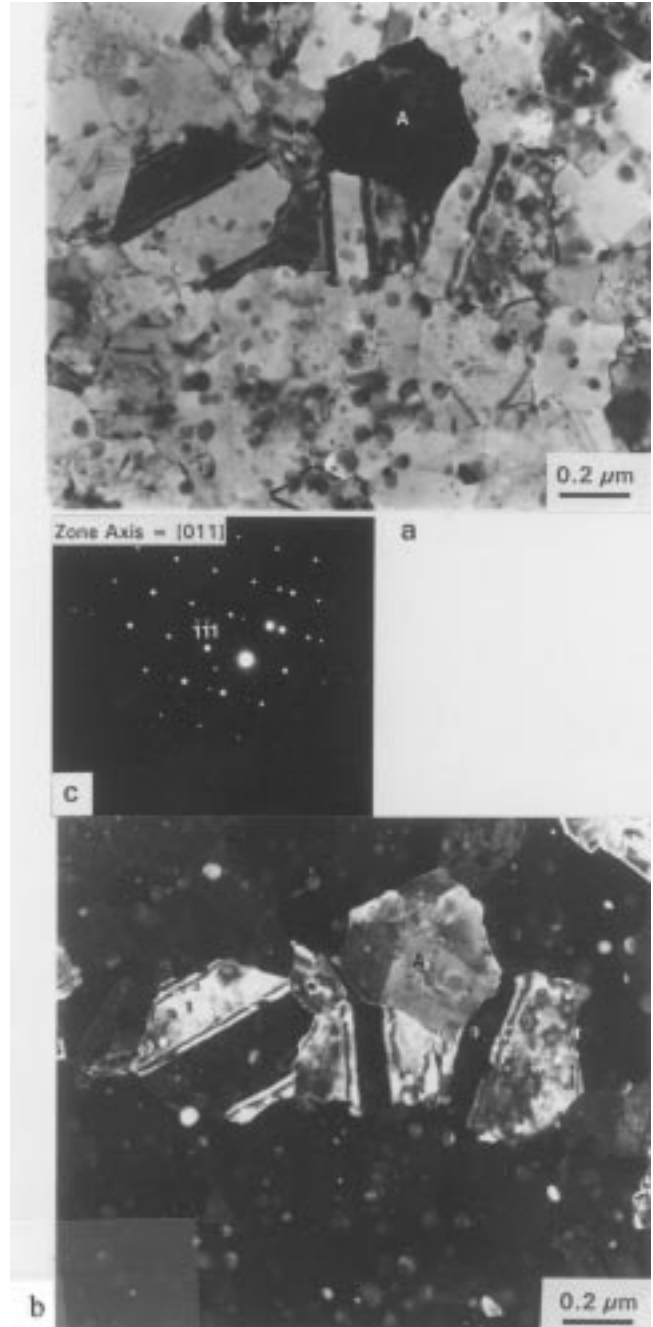


Fig. 11 TEM micrographs of a cluster of four closely aligned $\langle 110 \rangle$ grains in the untransformed region of a partially zone-annealed specimen

nucleation temperature. Quenching experiments in earlier studies (Ref 6) have shown that the nucleation of secondary recrystallization occurs at a temperature that is ~20 °C higher than the temperature at which the zoning interface migrates. The stability of 0.4 μm grains in this temperature range, which is above the zoning interface temperature, is likely to arise from the so-called Zener pinning by the oxide phase.

Normal grain growth refers to the increase in average grain size, but in the meantime an approximately uniform grain size distribution is maintained. The driving force for grain growth is the reduction in the total grain boundary energy that accompanies the reduction in grain-boundary area as the grain size increases. It was originally pointed out by Zener that grain growth can be inhibited by any second-phase inclusions present in the material. The mechanism of grain-growth inhibition is due to the reduction in grain-boundary area that occurs when a grain boundary intersects a particle.

According to Zener's original model (quoted by Smith in Ref 7), a limiting grain size is achieved when the driving force for grain growth and the dragging force of particles becomes equal and is given by:

$$R = \frac{4r}{3f} \approx D$$

where, for a roughly homogeneous grain structure, the grain curvature R is taken approximately equal to the mean grain diameter D (Ref 8) and r and f are the radius and volume fraction of the second phase particles, respectively. Taking the average radius of oxide particles as 5.5 nm and the volume fraction to be 0.025, one obtains a Zener pinned grain size of $D \approx 0.3 \mu\text{m}$, which is close to that observed.

The above calculations of Zener pinning are very approximate because, in the original theory, several parameters such as particle shape, interfacial energies, grain-boundary flexibility,

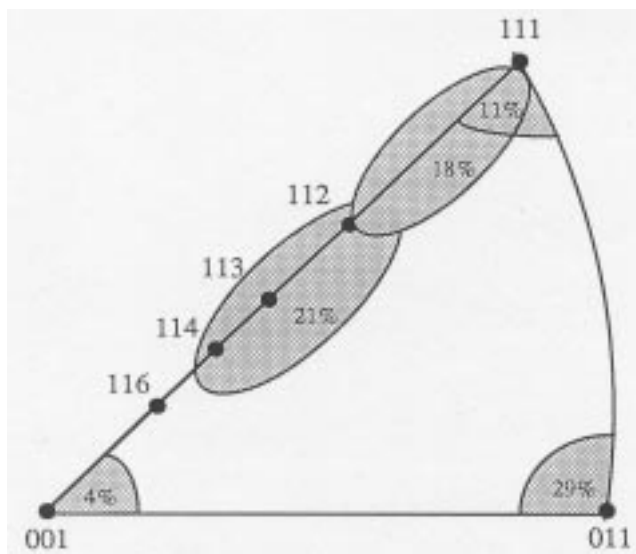
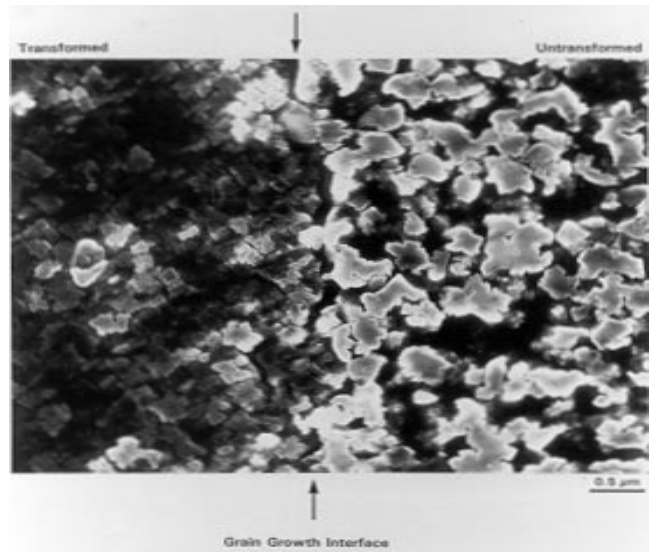
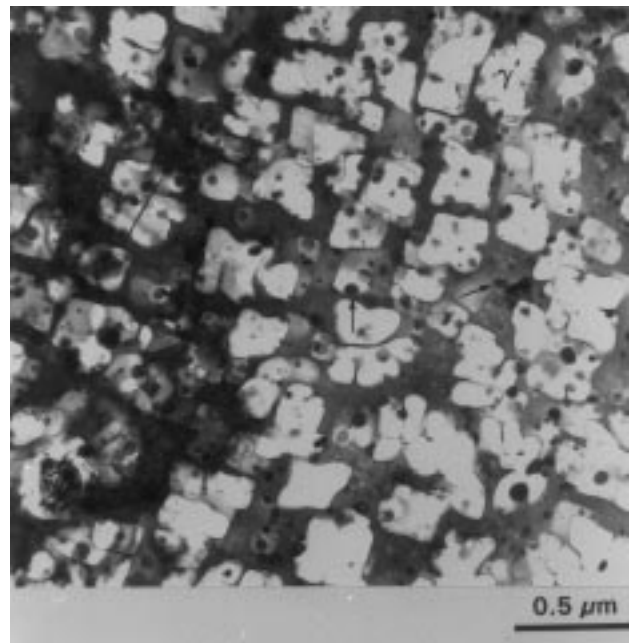


Fig. 12 Schematic diagram of standard triangle showing the texture (along extrusion axis) in a partially zone-annealed specimen near the transformation temperature

and the forces acting on the boundary were not taken into account. Louat (Ref 9) has made some modifications to the theory by giving due consideration to these important parameters. For the present material, a grain size (D_1) of 1.15 μm was obtained using a relationship given by Louat (for incoherent particles), which is much larger compared to the observed grain size.



(a)



(b)

Fig. 13 (a) SEM micrograph showing the γ morphology across the zoning interface in partially zone-annealed specimen. (b) TEM micrograph of recrystallized MA-6000 showing γ and the oxide dispersion

Louat also considered the interaction between particles and grain boundary and derived an expression for the extreme case where complete wetting occurs (i.e., fully coherent particles). A grain size (D_2) of 0.26 μm was obtained by using this relationship, which is approximately one-fourth of D_1 calculated earlier. This is also in accordance with Doherty's model (Ref 10), which predicts a four-fold increase in the resistance to grain-boundary migration when the particles are fully coherent.

The experimentally observed grain size (0.4 μm) is closer to D_2 , which accounts for particle-boundary interactions (i.e., considers coherency of particles with the matrix). This suggests that the oxide particles in the present material are at least partially coherent with the matrix. The coherency of oxide particles in alloy MA6000 has been confirmed by Mujahid and Martin (Ref 11) in some preliminary high-resolution electron microscopy (HREM) studies. Because the alloy is prepared by mechanical alloying, it would be thought that the oxide particles were incoherent with the matrix. In addition, Raghavan et al. (Ref 12) have found that the yttria dispersion is not stable, but transforms to various mixed Al/Y oxides during thermomechanical processing. Such reactions are likely to change the character of the oxide/matrix interface. High-resolution image in Fig. 14 shows one such oxide particle observed in an MA-6000 specimen quenched from above the γ -solvus temperature. Lattice continuity between the oxide and matrix is evident, implying the presence of a degree of coherency at the

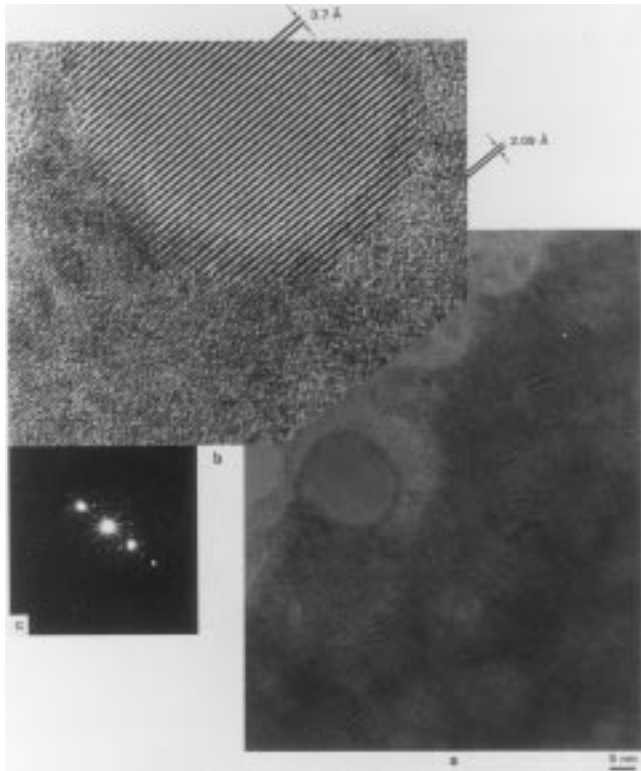


Fig. 14 (a) High-resolution TEM image showing an oxide particle in a large $\langle 110 \rangle$ grain. (b) Enlarged view of the particle matrix interface showing a degree of coherency. (c) Optical diffraction pattern showing spots from the matrix as well as from the oxide particles

interface. This will cause an increased Zener pinning force per unit area exerted by the particles on the grain boundaries, which in turn limits the grain size to around 0.4 μm .

4.2 Effect of Grain Reorientation

The increase in the population of $\langle 110 \rangle$ grains ahead of the zoning interface (Fig. 10) is relatively large in magnitude, approaching 36% at the interface (of rectangular bars) itself. Because the actual nucleation of secondary recrystallized grains occurs at up to 20 °C above the stable interface temperature, it is possible that reorientation of matrix grains may continue within this intermediate region, giving rise to an even higher population of $\langle 110 \rangle$ grains at the point of nucleation. The source of these oriented grains must therefore be plentiful, whether they are matrix grains lying more than 10° from a $\langle 110 \rangle$ direction or suitably oriented twins.

Grain Rotation. It is possible to distinguish between the two proposed models for grain reorientation by drawing comparisons between the number of $\langle 110 \rangle$ grains in an untilted foil and those in a foil tilted at 10° to the extrusion axis in which the grains oriented at 10 to 20° from a $\langle 110 \rangle$ direction may be identified. If reorientation is achieved by rotation and a cooperative diffusion process, there would be a substantial reservoir of grains lying in the 10 to 20° range from $\langle 110 \rangle$, requiring only a small rotation to lie within 10° of the recrystallization texture. Due to the extent of the diffusion processes involved in the rotation of a grain within a solid matrix, it is unlikely that the rotation of grains from outside this angular range would be energetically feasible. The population of $\langle 110 \rangle$ grains in the tilted foil would therefore be expected to exceed or at least equal that in the untilted foil if rotation constitutes the dominant reorientation mechanism. Table 1 shows, however, that there are no such grains available in the material, and as the foil normal is rotated further from the extrusion axis the population of potential $\langle 110 \rangle$ grains actually decreases. The alternative mode of reorientation—namely twin growth—must be operating, and this possibility is explored in more detail below.

Twin Growth. If a twin oriented with $\langle 110 \rangle$ direction parallel to the extrusion axis were to grow at the expense of the parent grain until the entire grain were consumed, this would effectively result in a grain reorientation toward $\langle 110 \rangle$. The population of $\langle 110 \rangle$ would therefore increase as the interface is approached, the rate of twin growth being enhanced by the associated increase in temperature. The driving force for this growth would be provided by the reduction in interfacial energy brought by replacing the high-energy grain boundary with the lower-energy configuration associated with a twin orientation.

The twinning transformation in a fcc material such as the matrix of MA-6000 is equivalent to a rotation of 60° around a $\langle 111 \rangle$ direction. In order to determine the orientation of a grain that would contain a twin oriented in the $\langle 110 \rangle$ direction, it is necessary to perform a “reverse twinning” operation, that is, a rotation of 180° about the $\langle 111 \rangle$ direction. The result of performing such a transformation can be illustrated using the stereographic projection described in Fig. 15, where it can be observed that (110) is mapped to a point lying between (113) and (115). It may be demonstrated using standard geometry

that this point corresponds to (114), because the $\langle 114 \rangle$ and $\langle 110 \rangle$ directions form the same angle with $\langle 111 \rangle$.

It is evident from the above calculations that an annealing twin lying in a $\langle 110 \rangle$ direction would be formed in a grain exhibiting a $\langle 114 \rangle$ orientation. Because the vast majority of matrix grains in the as-extruded material lie in the $\langle 001 \rangle$ to $\langle 111 \rangle$ band (Fig. 3), it is therefore reasonable to suggest that a sufficient number of suitably oriented twins would be available for growth in the as-received matrix to account for the observed reorientation phenomenon.

4.3 Secondary Recrystallization

Secondary recrystallization (or abnormal grain growth) can be initiated either by incomplete restriction of normal grain growth or by an inhomogeneous initial grain size distribution where some grains already have a size advantage, and therefore a driving force for a continued growth may exist (Ref 13). Gladman (Ref 14) has reviewed the abnormal grain growth that results from the presence of a few grains of sufficient size advantage to overcome the pinning forces of a particulate array. Gladman's model suggests that in a system where the particles give effective pinning of all grains, particle coarsening at elevated temperatures will progress to a stage where a single grain (possessing the largest size advantage) will be released.

Because the Gladman theory suggests a solutioning or coagulation of the pinning phases before the onset of abnormal grain growth, it cannot be applied directly to the present materials, which contain a stable oxide phase. Therefore, another approach for the initiation of secondary recrystallization is needed that is based on factors other than just the *size advantage*. More recently, Wörner, Romero, and Hazzledine (Ref 15) have taken into account the grain boundary *mobilities* and *energies* as well as the *size advantage* of a growing grain. They stressed that all three parameters are important in determining whether and to what extent abnormal grain growth occurs, and they have derived an expression to show their combined effect.

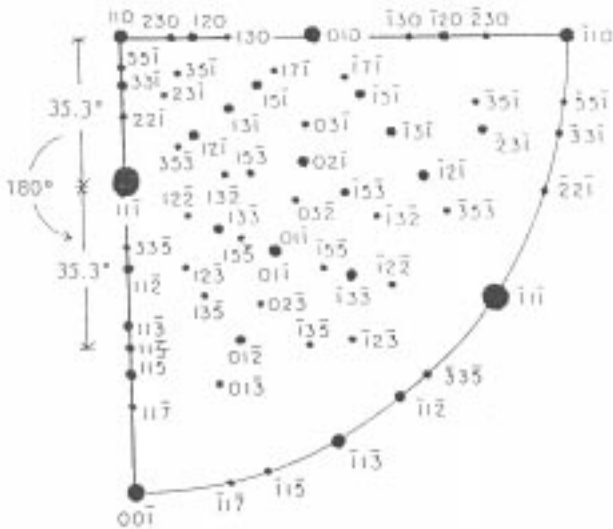


Fig. 15 Partial stereographic projection showing the “reverse-twinning” operation

Below the secondary recrystallization temperature, the grains in the current materials were observed to be completely pinned by the oxide particles to a size of approximately $0.4 \mu\text{m}$, and, therefore, a size advantage is *not* present initially.

The presence of small clusters of [110] grains (observed in TEM, Fig. 11) shows that the boundaries shared by these grouped grains would be of low misorientation and hence exhibit low grain boundary energy. Gore et al. (Ref 16) have derived an expression for the activation energy for unpinning a grain from interactions with second-phase particles. For a given dispersion, its magnitude is directly proportional to γ_a , the specific grain boundary energy, of the abnormally growing grain. Accordingly, the low misorientation boundaries between the closely aligned [110] grains, because of the low activation energy barrier, can unpin preferentially, providing a larger [110] grain. The interfaces within the groups of [110] grains thus provide an energy advantage for unpinning and can thus act as embryos to a (successful) nucleus, which in turn provides a size advantage.

In general, grain-boundary mobility increases as the misorientation between the grains increases (due to the more open structure of high angle boundaries, which provides faster diffusion paths). Because the [110] grains with a size advantage (potential nuclei) are embedded in a “matrix” that has grain orientations lying between $\langle 100 \rangle$ and $\langle 111 \rangle$, there is a high probability of their having many high-angle boundaries around them. Those interfaces with a higher angular misorientation may also possess a mobility advantage and would grow by consuming the “matrix” grains.

4.4 Implication of Grain Reorientation Process on Recrystallization

The implications of this reorientation process lie in the nature of the final recrystallized microstructure and hence with the ultimate properties of the material. The effect of an increased $\langle 110 \rangle$ grain population at the point of nucleation of secondary recrystallized grains is to increase the total number of nuclei. This results in the growth of an increased number of grains and leads to a finer recrystallized structure. The scale of this microstructure could therefore potentially be controlled by variation of the speed at which the as-extruded material was brought up to the zone-annealing temperature. The rate of twin growth is reliant on the thermal conditions; should there be insufficient time for the reorientation process to proceed, the number of $\langle 110 \rangle$ grains would be reduced, giving rise to fewer nuclei and a coarser recrystallized structure. Conversely, a long period of pretreatment would lead to a fully developed reorientation process, and the microstructure of the resultant material would be effectively refined.

5. Conclusions

- Grains with maximum aspect ratio along the extrusion axis can be produced by zone annealing of extruded bars.
- The grains remain Zener pinned (to a size of about $0.4 \mu\text{m}$) by the oxide dispersion up to the secondary recrystallization temperature.

- The oxide particles are partially coherent with the matrix, giving rise to an increased resistance to grain-boundary migration during annealing.
- The reorientation of grains ahead of the secondary recrystallization interface in MA-6000 during the zone-annealing process is thought to be brought about by the growth of annealing twins with <110> texture, which occurs within grains exhibiting a <114> texture.
- There are insufficient grains with <110> texture to give rise to the increased texture by grain-rotation process.
- The results suggest that the final secondary recrystallized grain size may be controlled by the degree of this reorientation.

References

1. J.S. Benjamin, *New Materials by Mechanical Alloying Techniques*, E. Arzt and L. Schultz, Ed., DGM e.V., Oberursel, Germany, 1989, p 3-18
2. E. Arzt, *New Materials by Mechanical Alloying Techniques*, E. Arzt and L. Schultz, Ed., DGM e.V., Oberursel, Germany, 1989, p 185-200
3. C.P. Jongenburger and R.F. Singer, *New Materials by Mechanical Alloying Techniques*, E. Arzt and L. Schultz, Ed., DGM e.V., Oberursel, Germany, 1989, p 157
4. J.M. Marsh and J.W. Martin, *Mater. Sci. Technol.*, Vol 7, 1991, p 183-188
5. A. Tekin and J.W. Martin, *Metallography*, Vol 22, 1989, p 1
6. M. Mujahid and J.W. Martin, *Mater. Sci. Technol.*, Vol 10, 1994, p 703-710
7. C.S. Smith, *Trans. AIME*, Vol 175, 1948, p 348
8. R.W. Cahn, *Recrystallization, Grain Growth and Textures*, American Society for Metals, 1966, p 99
9. N. Louat, *Philos. Mag.*, Vol A47 (No. 6), 1983, p 903
10. R.D. Doherty, *Met. Sci.*, Vol 16, 1982, p 1
11. M. Mujahid and J.W. Martin, *J. Mater. Sci. Lett.*, Vol 13, 1994, p 153-155
12. M. Raghavan, J.W. Steeds, and R.A. Petrovic-Luton, *Metall. Trans. A*, Vol 13A, 1982, p 953
13. V. Randle, B. Ralph, and N. Hansen, *Annealing Processes*, N. Hansen, D.J. Jensen, T. Leffers, and B. Ralph, Ed., Riso National Laboratory, Roskilde, Denmark, 1986, p 123
14. T. Gladman, *Proc. R. Soc.*, Vol A294, 1966, p 298
15. C.H. Wörner, S.R. Romero, and P.M. Hazzledine, *J. Mater. Res.*, Vol 6 (No. 8), 1991, p 1773
16. M. J. Gore, M. Grujicic, G.B. Olson, and M. Cohen, *Acta Metall.*, Vol 37, 1989, p 2849